Topology Optimal Design of NRD Guide Devices Using Function Expansion Method and Evolutionary Approaches

Topology Optimal Design of NRD Guide Devices Using Function Expansion Method and Evolutionary Approaches

Naoya HIEDA[†], *Student Member*, Keita MORIMOTO[†], Akito IGUCHI[†], *Members*,
Yasuhide TSUJI[†a)], *Senior Member*, and Tatsuya KASHIWA[††], *Fellow*

SUMMARY   In order to increase communication capacity, the use of millimeter-wave and terahertz-wave bands are being actively explored. Non-radiative dielectric waveguide known as NRD guide is one of promising platform of millimeter-wave integrated circuits thanks to its non-radiative and low loss nature. In order to develop millimeter wave circuits with various functions, various circuit components have to be efficiently designed to meet requirements from application side. In this paper, for efficient design of NRD guide devices, we develop a topology optimal design technique based on function-expansion-method which can express arbitrary structure with arbitrary geometric topology. In the present approach, recently developed two-dimensional full-vectorial finite element method (2D-FVFEM) for NRD guide devices is employed to improve computational efficiency and several evolutionary approaches, which do not require appropriate initial structure depending on a given design problem, are used to optimize design variables, thus, NRD guide devices having desired functions are efficiently obtained without requiring designer's special knowledge.

key words: NRD guide device, finite element method, topology optimization, function expansion method, evolutionary approach

1. Introduction

With the rapid spread of a variety of communication services and increase of wireless communication traffic, the use of millimeter-wave and terahertz-wave bands are being actively explored to increase communication capacity. Non-radiative dielectric waveguide known as NRD guide [1] is one of promising platform of millimeter-wave integrated circuit thanks to its non-radiative and low loss nature. Although several kinds of NRD guide devices have been reported so far [1]–[13], a well established design methodology for realizing optimal device having arbitrary given target property has not developed yet. In order to develop millimeter wave circuits with various functions, various circuit components have to be efficiently designed to meet requirements from application side.

In recent years, optimal design techniques have been intensively studied for developing high performance electromagnetic devices [14]. These optimization techniques are roughly categorized into size optimization, shape optimization, and topology optimization. Among them, topol-

ogy optimization has highest design freedom and can obtain arbitrary structure with arbitrary geometric topology [14]–[25]. Therefore, topology optimization has a possibility to dramatically improve device performance beyond human knowledge and efficient topology optimization method for NRD devices is expected to be developed.

In this paper, we develop a topology optimal design approach based on function-expansion-method [17] for designing NRD guide devices without requiring designer's profound knowledge and experience. In our approach, by employing evolutionary approaches to optimize design variables, appropriate initial structure depending on a given design problem is not required and NRD guide devices with desired functions are efficiently obtained. A lot of kinds of evolutionary approaches have been proposed and developed so far [26]–[29], however, the performances of these approaches often depend on design problems. In this paper, we employ four kinds of evolutionary approaches, genetic algorithm (GA) [26], differential evolution (DE) [27], hybrid firefly algorithm (HFA) [28], and harmony search (HS) [29], and compare the results by these approaches. In addition, we employ recently developed two-dimensional full-vectorial finite element method (2D-FVFEM) for NRD guide devices [30] to improve design efficiency. Using our 2D-FVFEM, NRD guide devices having three-dimensional structure can be rigorously analyzed in two-dimensional space if the dielectric between two metal plates is invariant along the perpendicular direction to two metal plates. Therefore, efficient simulation without requiring large computational resources has become available and the overall design efficiency can be dramatically improved.

In Sect. 2, we describe our topology optimization framework. The numerical expression in design region, four kinds of evolutionary approaches to optimize design variables, and the formulation of 2D-FVFEM for NRD guide are briefly described. Then, we show some design examples and give some discussions in Sect. 3 and summarize our results in Sect. 4.

2. Function-Expansion-Based Topology Optimization of NRD Guide Devices

2.1 Design Problem of NRD Guide Devices

Figure 1 shows an image of millimeter-wave circuit based on NRD guide and circuit components. We consider a de-
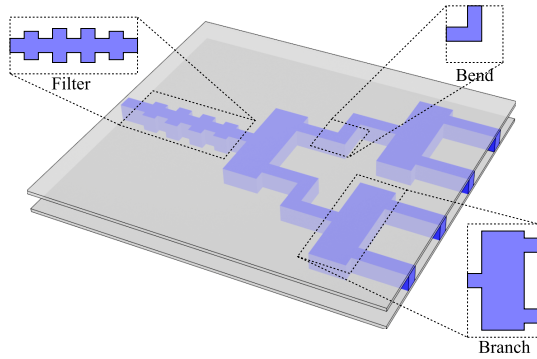
Fig. 1 An image of millimeter-wave circuit.
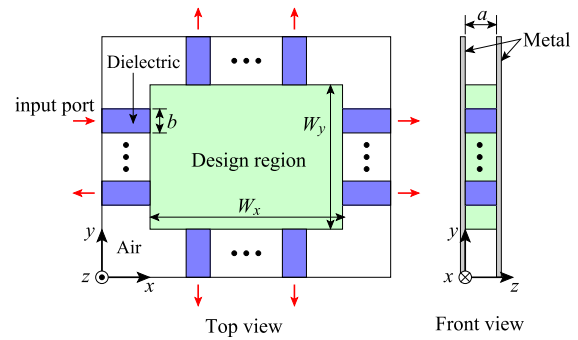
Fig. 2 Design model of a component of NRD circuit.

Fig. 3 An image of function-expansion-based representation of device structure.

sign problem of NRD guide devices as shown in Fig. 2. The fixed structural parameters in our design are set to be $a = 2.25$ mm, $b = 2$ mm, and computational domain is surrounded by perfectly matched layer (PML) with the thickness of $d_{PML} = 5$ mm [31], [32]. An incidence of LSM_{01} mode with around 60 GHz to port 1 is considered. The relative permittivities of air and dielectric are $\varepsilon_{air} = 1$ and $\varepsilon_d = 2.2$, respectively. Number and position of input and output ports are set depending on a design problem. The structure in design region with size of $W_x \times W_y$ is optimized to achieve a desired transmission property. We assume that the structure of the dielectric along the z-direction is invariant between two metal plates.

2.2 Function Expansion Method for Expressing Device Structure

In order to optimize a device structure with a desired property, a structure in the design region is usually expressed by a large number of numerical design variables. For this numerical representation, several kinds of approaches have been proposed so far. In this paper, we employ the function expansion method [17] which is easy to express arbitrary structure with arbitrary geometric topology by a relatively small number of design variables. In the function expansion method, a relative permittivity distribution in the design region is expressed as follows:

$$\varepsilon_r(x, y) = \varepsilon_{air} + (\varepsilon_d - \varepsilon_{air})H(w(x, y)) \quad (1)$$

$$w(x, y) = \sum_{m=1}^{N_d} c_m f_m(x, y) \quad (2)$$

where $H(w)$ is Heaviside step function to be used for binarizing material constant, N_d is the number of design variables, $f_m(x, y)$ is m-th basis function, and coefficients c_m $(m = 1, 2, \cdots, N_d)$ are the design variables in this optimization problem. Various functions can be used as $f_i(x, y)$ [20]. We will give the specific form of $f_i(x, y)$ when we will show actual numerical examples. Material boundaries which define device structure are obtained by zero-contour of the function $w(x, y)$, as shown in Fig. 3.
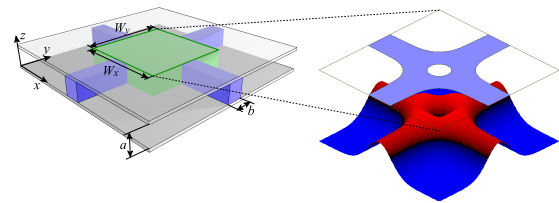
2.3 Evolutionary Methods for Optimizing Design Variables

In this topology optimization, we employ four kinds of evolutionary algorithms to optimize the design variables because these approaches show relatively good performance in our previous design problems of plasmonic devices. In the followings, we briefly explain each evolutionary method.

2.3.1 Genetic Algorithm (GA)

Genetic Algorithm (GA) is one of popular evolutionary approaches and is widely used. In addition, various types of variants have been developed so far. GA is based on genetic process, such as, crossover between selected parents and mutation. In this paper, both elite selection and ranking selection are employed to select parents. From the selected parents $(\boldsymbol{x}_{p_1}, \boldsymbol{x}_{p_2})$, the i-th design variable of children $(\boldsymbol{x}_c)$ in the next generation is generated as follows:

$$x_{c,i} = \begin{cases} Cx_{p_1,i} + (1 - C)x_{p_2,i} & (C_m > R_m) \\ x_{i,\min} + (x_{i,\max} - x_{i,\min})C & (\text{otherwise}) \end{cases} \quad (3)$$

where $C = U(0, 1)$, $C_m = U(0, 1)$, $U(a, b)$ is a function which returns a random number in $[0, 1]$. R_m is a mutation rate, and $x_{i,\min}$ and $x_{i,\max}$ are the minimum and maximum values of the i-th design variable, respectively. R_m is set to be $R_m = 0.03$ in the following optimization.

2.3.2 Differential Evolution (DE)

In DE algorithm, children $(\boldsymbol{x}_c)$ in the next generation is generated by crossover between basis parent $(\boldsymbol{x}_b)$ and mutated

parent (x_m). The mutated parent is generated from randomly selected three parents (x_{p_1}, x_{p_2}, x_{p_3}). The mutated parent and child in the next generation are generated as follows:

$$x_m = x_{p_1} + F(x_{p_2} - x_{p_3}) \tag{4}$$

$$x_{c,i} = \begin{cases} x_{m,i} & (C > 0.5) \\ x_{b,i} & \text{(otherwise)} \end{cases} \tag{5}$$

where $C = U(0, 1)$ and F is a scale factor and set to be $F = 0.7$ in the following optimization. The search space size depends on differential vectors, then, transition from global search to local search is readily realized in DE search process.

2.3.3 Hybrid Firefly Algorithm (HFA)

Hybrid firefly algorithm (HFA) is a hybrid scheme with the firefly algorithm (FA) and DE. In order to generate children in the next generation, individuals are divided into two subgroups and one is updated by DE and the other is updated by the FA. After that, two subgroups are mixed with each other and regrouped.

The FA is based on the fact that each firefly is attracted to all the superior ones. The updating formula of i-th firefly at n-th step in the optimization is expressed as follows:

$$x'_i = x_i + \sum_j H(\beta_{0,j} - \beta_{0,i})\beta_{0,j}e^{-\gamma r_{ij}^2}(x_j - x_i)$$
$$+ \alpha\delta^n\varepsilon \tag{6}$$

where $\beta_{0,k}$ is an attractiveness of k-th firefly, r_{ij} is a distance from x_i to x_j, γ is a light absorption coefficient, α is a scale factor, δ is a damping coefficient, and ε is a vector of random number whose value lies in $[-1, 1]$. In this optimization, $\gamma = 1/(4N_d)$, $\alpha = 0.1$, and $\delta = 0.99$ are used where N_d is the number of design variables.

2.3.4 Harmony Search (HS)

Harmony search is a scheme inspired by the improvisation process of jazz musicians. A new harmony is generated through selection and tuning process. Each design variable is selected from harmony memory, in which past relatively good harmonies are stored. The selected harmony is tuned or replaced by a random number with a certain probability. The new harmony x_h^{new} is generated as follows:

$$x_{h,i}^{\text{new}} = \begin{cases} x_{i,\min} + (x_{i,\max} - x_{i,\min})C \\ \qquad (C_h < (1 - R_{\text{hmcr}})) \\ x_{p_i,i} + \Delta \quad (C_h < (1 - R_{\text{hmcr}}) + R_{\text{hmcr}}R_{\text{par}} \\ x_{p_i,i} \qquad \text{(otherwise)} \end{cases} \tag{7}$$

where $C_h = U(0, 1)$, $C = U(0, 1)$, $\Delta = \alpha_{\text{BW}}U(-1, 1)$, R_{hmcr} is a harmony memory considering rate, R_{par} is a pitch adjusting rate, and α_{BW} is a bandwidth. In the following optimization, $R_{\text{hmcr}} = 0.98$, $R_{\text{par}} = 0.3$ is used, and α_{BW} is determined by difference value between arbitrary selected two harmonies.

2.4 Efficient Finite Element Analysis for NRD Guide Devices

In order to realize efficient optimization scheme, to employ highly efficient and highly accurate numerical simulation technique is one of crucial issues. In our recent work, we have developed a novel 2D-FVFEM for analyzing NRD guide devices [30]. In our simulation approach, when the structure between two metal plates is invariant along the perpendicular direction to the metal, NRD guide devices with three-dimensional structure can be rigorously analyzed in two-dimensional framework. Using this formulation, efficient simulation without requiring large computational resources has become available. The finite element formulation is briefly described and actual expression for calculating transmission power in each LSM and LSE mode is also derived.

Propagating behavior of millimeter-wave in NRD guide device is described by the following vector wave equation:

$$\nabla \times (\varepsilon_r^{-1}\nabla \times H) - k_0^2 H = 0 \tag{8}$$

where H is a magnetic field vector and k_0 is free-space wavenumber. Considering boundary conditions on metal plates, we can express each component of H is expressed as follows:

$$H_\xi = \psi_\xi(x, y)\cos(\pi z/a) \qquad (\xi = x, y) \tag{9}$$
$$H_z = \psi_z(x, y)\sin(\pi z/a) \tag{10}$$

Substituting (9) and (10) into the functional of (8), discretizing xy-plane into hybrid edge/nodal triangular elements [33], [34], and integrating the functional in three-dimensional space, we can get the following linear equation:

$$\left([K] - k_0^2[M]\right)\{\psi_z\} = \{u\} \tag{11}$$

where $[K]$ and $[M]$ are the finite element matrices and $\{u\}$ are the vector related to an incidence condition. The actual expression of these matrices and vector can be referred in [30]. In this formulation, z-dependence of H disappear by being taken integral in the z-direction.

In order to calculate modal power of each LSM mode and LSE mode, first, overlap integral with normalized modal field is calculated to obtain modal amplitude as follows:

$$a_{\text{LSM}_{m1}} = \int_\Gamma \varepsilon_r^{-1}\Psi_{z,\text{LSM}_{m1}}^*\psi_z d\Gamma \tag{12}$$

$$a_{\text{LSE}_{m1}} = \int_\Gamma \Psi_{t,\text{LSE}_{m1}}^*\psi_t d\Gamma \tag{13}$$

where t express the transverse direction to the propagating direction and perpendicular to the metal plates, $\Psi_{z,\text{LSM}_{m1}}$ and $\Psi_{t,\text{LSE}_{m1}}$ are the normalized modal fields of LSM_{m1} and LSE_{m1} modes, respectively. After obtaining model amplitudes $a_{\text{LSM}_{m1}}$ and $a_{\text{LSE}_{m1}}$ for LSM and LSE modes, respectively, the normalized modal power for LSM_{m1} and LSE_{m1}

respectively are calculated as follows:

$$P_{\text{LSM}_{m1}} = \frac{\beta_{\text{LSM}_{01}}\left\{(\pi/a)^2 + \beta^2_{\text{LSM}_{m1}}\right\}}{\beta_{\text{LSM}_{m1}}\left\{(\pi/a)^2 + \beta^2_{\text{LSM}_{01}}\right\}}\left|a_{\text{LSM}_{m1}}\right|^2 \tag{14}$$

$$P_{\text{LSE}_{m1}} = \frac{k_0^2 \beta_{\text{LSM}_{01}} \beta_{\text{LSE}_{m1}} \left|a_{\text{LSE}_{m1}}\right|^2}{\left\{(\pi/a)^2 + \beta^2_{\text{LSM}_{01}}\right\}\left\{(\pi/a)^2 + \beta^2_{\text{LSE}_{01}}\right\}} \tag{15}$$

where $\beta_{\text{LSM}_{m1}}$ and $\beta_{\text{LSE}_{m1}}$ are the propagation constants of LSM_{m1} and LSE_{m1} modes, respectively.

3. Design Examples

3.1 Branching Waveguide

We consider a design problem of branching device as shown in Fig. 4. The separation of two output waveguides is set to 10 mm for getting enough separation. In order to realize a compact branch, the design region size is set to $W_x \times W_y = 6$ mm $\times 18$ mm. LSM_{01} mode with frequency of $f = 60$ GHz is assumed as an incident wave. In this paper, we define the structure expressing function, $w(x, y)$, in the function expansion method as follows:

$$w(x, y) = \sum_{m=-N_x}^{N_x-1} \sum_{n=0}^{N_y-1} \{a_{mn}\cos\theta_{mn} + b_{mn}\sin\theta_{mn}\}, \tag{16}$$

$$\theta_{mn} = \frac{2\pi m}{L_x}x + \frac{2\pi n}{L_y}y. \tag{17}$$

where a_{mn} and b_{mn} are the design variables in the present topology optimization. In order to avoid undesired periodicities, the fundamental periods of Fourier series should be greater than the design region sizes. Thus, we set $L_x = 1.1W_x$, $L_y = 1.1W_y$. N_x and N_y are better to be smaller for avoiding complicated fine structures in optimized devices, thus we set $N_x = 2$ and $N_y = 4$ in this design example. We have to increase the number of design variables if the design freedom is insufficient to achieve desired characteristics. In addition, the structural symmetry condition along the y-direction is imposed to obtain symmetrical outputs. An objective function of this design problem is set as follows:
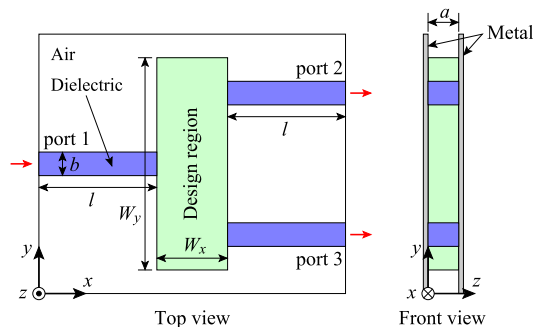
$$\text{Minimize } C = 1 - 2\left|S_{21}^{\text{LSM}_{01}}\right|^2 \tag{18}$$

where S_{i1}^{MODE} denotes scattering parameter into i-th port as a given "MODE" when LSM_{01} mode is launched into port 1. Because of the structural symmetry along y-direction, $S_{31}^{\text{LSM}_{01}} = S_{21}^{\text{LSM}_{01}}$. Therefore, C corresponds to an insertion loss including a reflection and a converted LSE mode power. Four optimization methods described in the previous section are applied and compared with each other.

Figure 5 shows the convergence behavior in each optimization method. Although GA and HFA seem to show better design performance, every optimization method can obtain sufficient device performance with less insertion loss than -20 dB. Figure 6 shows the frequency characteristic, optimized structure, and propagating field at $f = 60$ GHz for each optimization result. We can see that the optimized structures are greatly different with each other. It is considered that this difference is not due to the difference in the optimization method, but to the difference in the initial pop-
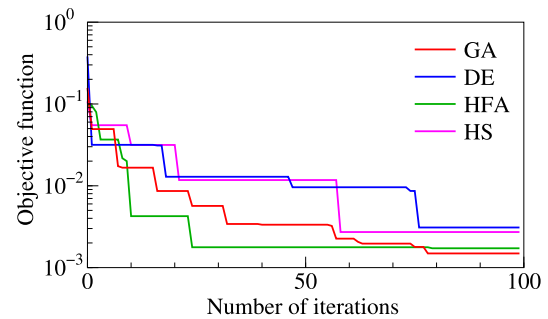

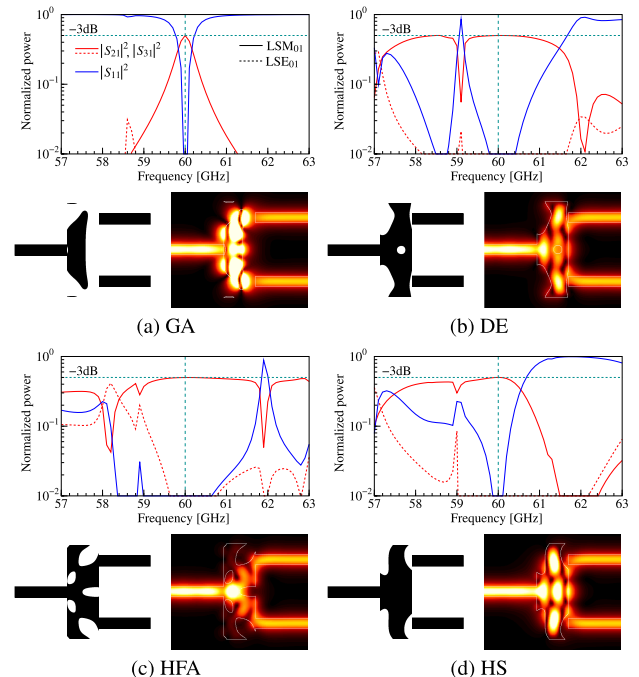**Fig. 5** Convergence behavior of each optimization method for optimization of branching waveguide at $f = 60$ GHz.

(a) GA   (b) DE

(c) HFA   (d) HS

Fig. 6 Optimized results of branching waveguide at $f = 60$ GHz.

Fig. 4 Design model of branching waveguide.
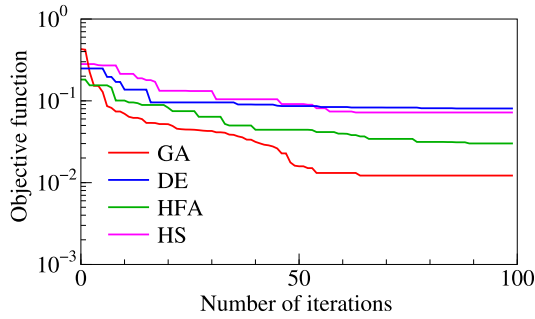
Fig. 7 Convergence behavior of each optimization method for optimization of wideband branching waveguide.

Fig. 9 Design model of bending waveguide.

(a) Frequency characteristic

(b) Optimized Structure   (c) Propagating field
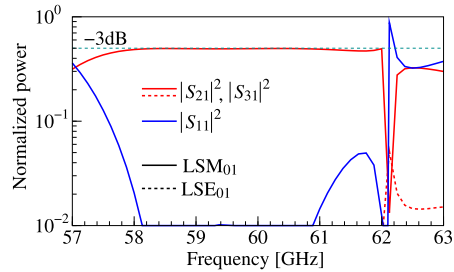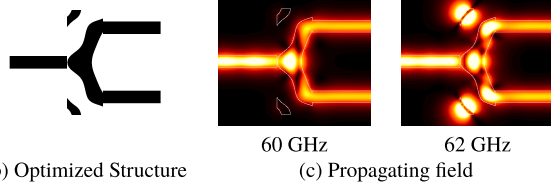
Fig. 8 Optimized result of wideband branching waveguide by GA.

Fig. 10 Convergence behavior of each optimization method for optimization of bending waveguide.

tion band than those designed only at 60 GHz.

3.2 Bending Waveguide

Next, we consider a design example of bending waveguide as shown in Fig. 9. The size of design region is set to be $W_x \times W_y = 8\,\text{mm} \times 8\,\text{mm}$. The parameters in (16) and (17) are set to be $L_x = 1.2W_x$, $L_y = 1.2W_y$, $N_x = 3$, and $N_y = 3$. An objective function is defined as follows:

$$\text{Minimize } C = \frac{1}{N_f} \sum_{i=1}^{N_f} \left(1 - \left|S_{21}^{\text{LSM}_{01}}(f_i)\right|^2\right)^2 \qquad (20)$$

Operation frequency band is assumed to be 58 GHz~62 GHz and we set $N_f = 5$ and $f_i = (i + 57)$ GHz. Figure 10 shows the convergence behavior in four different optimizations. In this design, HS achieved the best result in the view point of the objective function. Figure 11 shows the optimized result by HS. We can see that the sharp dip is observed in the frequency characteristic. The frequency where transmission drops is not considered in this optimization, therefore, we cannot avoid these phenomena in the present objective function. The non-radiative nature of NRD guide is an advantage for realizing low loss devices. On the other hand, this sometimes cause unwanted resonance and make the optimal design difficult. Figure 12 shows the optimized result by HFA. Such an unwanted resonance is not observed in this optimized result although average transmission is slightly lower than that obtained by HS.

ulation whose individuals are randomly generated. Convergence behavior also partly depends on the initial population. From these results, we can see that a lot of optimal structures with almost same device performance exist in the current optimization condition. On the other hand, the frequency characteristics are dramatically different with each other because the optimization is carried out only at $f = 60$ GHz. The results by HFA and DE have a relatively wider operation frequency band, while the results by GA has an extremely narrow operation frequency band. Therefore, we have to design the branching waveguide considering wideband operation.

In order to achieve wideband operation, the objective function is modified as follows:

$$\text{Minimize } C = \frac{1}{N_f} \sum_{i=1}^{N_f} \left\{1 - 2\left|S_{21}^{\text{LSM}_{01}}(f_i)\right|^2\right\}. \qquad (19)$$

Here, considering an operation within $f = 58 \sim 62$ GHz, we set $N_f = 5$ and $f_i = (i + 57)$ GHz. The other design settings are the same as the previous ones.

Figure 7 shows the convergence behavior in four different optimizations. In this design, GA achieved the best results. Figure 8 shows the optimized result by GA. We can see that the obtained branching waveguide has wider opera-
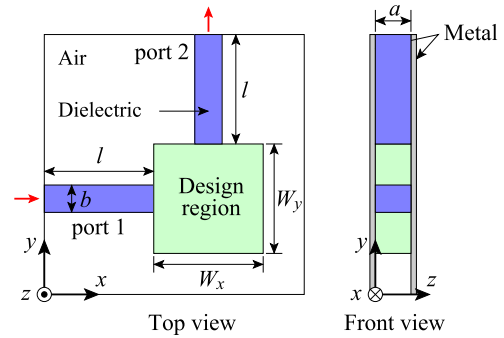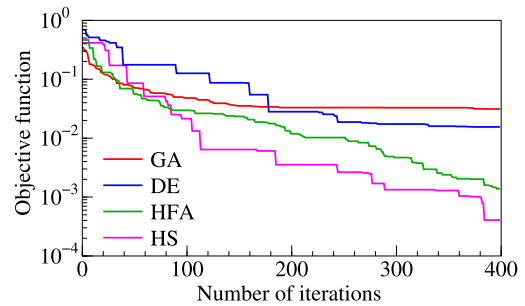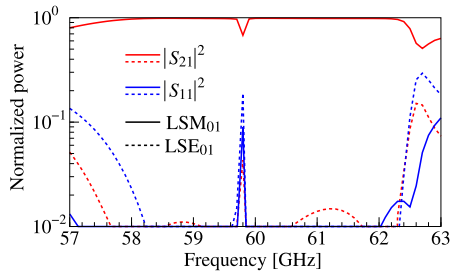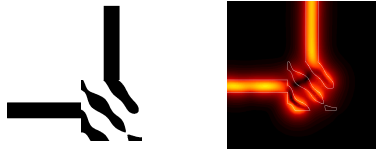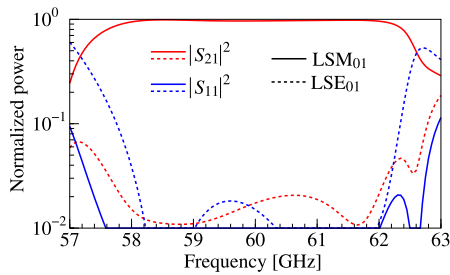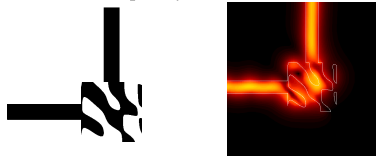
(a) Frequency characteristic

(b) Optimized Structure   (c) Propagating field

Fig. 11 Optimized result of bending waveguide by HS.

(a) Frequency characteristic

(b) Optimized Structure   (c) Propagating field

Fig. 12 Optimized result of bending waveguide by HFA.

3.3 Bandpass Filter

Finally, we consider a design example of bandpass filter as shown in Fig. 13. The size of design region is set to be $W_x \times W_y$ = 20 mm × 6 mm. The parameters in (16) and (17) are set to be $L_x = 1.2W_x/2$, $L_y = 1.2W_y/2$, $N_x = 5$, and $N_y = 2$ and symmetry conditions are imposed along the x- and y-directions. The transmission band is assumed to be 60 ± 0.2 GHz and an objective function is defined as follows:

$$\text{Minimize } C = \frac{1}{N_f} \sum_{i=1}^{N_f} \left(P(f_i) - \left| S_{21}^{\text{LSM}_{01}}(f_i) \right|^2 \right)^2 \quad (21)$$

where $N_f = 31$ and frequencies are considered at intervals of 0.2 GHz within 57.0 ~ 59.4 GHz and 60.6 ~ 63.0 GHz, and at intervals of 0.1 GHz within 59.8 ~ 60.2 GHz. $P(f_i)$ is set to be 1 within the transmission band and otherwise 0. In this design problem, we consider a lot of frequencies in the objective function to suppress undesired resonance
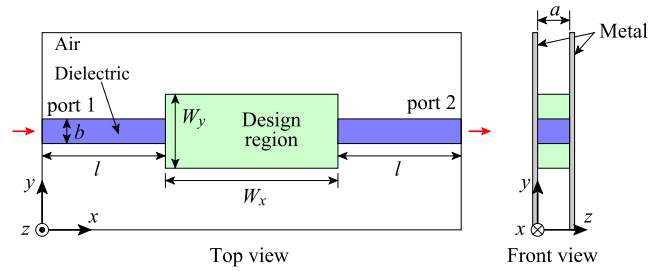

Top view   Front view
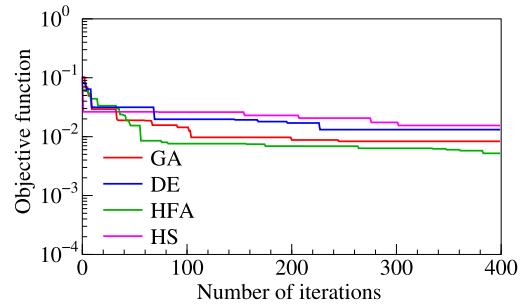
Fig. 13 Design model of bandpass filter.

Fig. 14 Convergence behavior of each optimization method for optimization of bandpass filter.

(a) Frequency characteristic

(b) Optimized structure   (c-1) Propagating field (59 GHz)

(c-2) Propagating field (60 GHz)   (c-3) Propagating field (61 GHz)
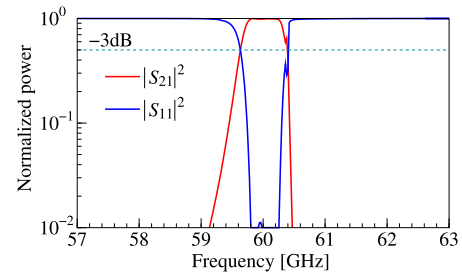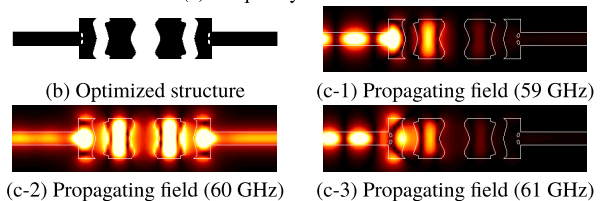
Fig. 15 Optimized result of wideband branching waveguide by HFA.

transmissions because such undesired transmissions are observed in our preliminary optimization with a small number of frequencies

Figure 14 shows the convergence behavior in four different optimizations. In this design, HFA achieved the best result in the view point of the objective function. Figure 15 shows the optimized result by HFA. We can see that flat top transmission band is obtained around 60 GHz.

4. Conclusion

In this paper, we proposed the function-expansion-based topology optimization of NRD guide devices. In our ap-

proach, characteristics of a given device can be efficiently and rigorously simulated by 2D-FVFEM without requiring 3D analysis and design variables are optimized by an evolutionary algorithm. In this paper, four different optimization techniques are investigated and compared with each other. Although we cannot say which optimization technique is better in the proposed topology optimization than the others, some of them or all of them could achieve sufficient optimization in every design problem. In general, the convergence of optimization is faster when the number of design variables is smaller. It is also shown that the function expansion method can express arbitrary device structure with a relatively small number of design variables. We are now considering to develop more robust optimization technique combining these optimization techniques. In addition, in the design of NRD guide devices, undesired frequency characteristics are sometimes observed unlike the optimization in photonic devices because the device property is evaluated at discrete frequencies in the objective function. This phenomena is originated from the existence of strong resonance due to the intrinsic non-radiative nature of NRD guide. In order to avoid these undesired frequency characteristics, some improvement may be required in more sophisticated design problems. We are thinking that an optimization method utilizing time-domain analysis is also one candidate to overcome this problem.

Acknowledgments

References

[1] T. Yoneyama and S. Nishida, "Nonradiative dielectric waveguide for millimeter-wave integrated circuits," IEEE Trans. Microw. Theory Tech., vol.MTT-29, no.11, pp.1188–1192, Nov. 1981.

[2] T. Yoneyama and S. Nishida, "Nonradiative dielectric waveguide T-junctions for millimeter-wave applications," IEEE Trans. Microw. Theory Tech., vol.MTT-33, no.11, pp.1239–1241, Nov. 1985.

[3] T. Yoneyama, S. Nishida, and I. Tamaki, "Analysis and measurements of nonradiative dielectric waveguide bends," IEEE Trans. Microw. Theory Tech., vol.MTT-34, no.8, pp.876–882, Aug. 1986.

[4] T. Yoneyama, "Millimeter-wave integrated circuits using nonradiative dielectric waveguide," IEICE Trans. Electron. (Jananese Edition), vol.J73-C-I, no.3, pp.87–94, March 1990.

[5] K. Wu and L. Han, "Hybrid integration technology of planar circuits and NRD-guide for cost-effective microwave and millimeter-wave applications," IEEE Trans. Microw. Theory Tech., vol.45, no.6, pp.946–954, June 1997.

[6] F. Boone and K. Wu, "Mode conversion and design consideration of integrated nonradiative dielectric (NRD) components and discontinuities," IEEE Trans. Microw. Theory Tech., vol.48, no.4, pp.482–492, April 2000.

[7] F. Kuroki, K. Wada, and T. Yoneyama, "Low-loss and small-sized NRD guide ring resonators and their application to channel dropping filter at 60 GHz," IEICE Trans. Electron., vol.E86-C, no.8, pp.1601–1606, Aug. 2003.

[8] J.Y. Lee, J.H. Lee, C.H. Im, H.S. Kim, K. Choi, and H.-K. Jung, "Selection of proper modes of an NRD guide using a perturbing boundary," IEEE Trans. Magnet., vol.39, no.3, pp.1246–1249, May 2003.

[9] D. Li, Y. Cassivi, P. Yang, and K. Wu, "Analysis and design of bridged NRD-guide coupler for millimeter-wave applications," IEEE Trans. Microw. Theory Tech., vol.53, no.8, pp.2546–2551, Aug. 2005.

[10] F. Kuroki, K. Makoto, and T. Yoneyama, "A transition between NRD guide and microstrip line at 60 GHz," IEICE Trans. Electron., vol.E88-C, no.10, pp.1968–1972, Oct. 2005.

[11] Y. Kamo, K. Munetou, and F. Kuroki, "Transmission loss evaluation of 94GHz NRD guide toward THz-band dielectric integrated circuits," 2016 IEEE Int. Symp. Radio-Frequency Integration Technology (RFIT), Aug. 2016.

[12] E. Polat, R. Reese, M. Jost, C. Schuster, M. Nickel, R. Jakoby, and H. Maune, "Tunable liquid crystal filter in nonradiative dielectric waveguide technology at 60 GHz," IEEE Microw. Wireless Compon. Lett., vol.29, no.1, Jan. 2019.

[13] U. Schmid and W. Menzel, "A 24 GHz microstrip antenna array with a non-radiative dielectric waveguide (NRD-guide) feeding network," 11th Int. Symp. Antenna Technology and Applied Electromagnetics (ANTEM 2005), pp.1–4, July 2005.

[14] S. Molesky, Z. Lin, A.Y. Piggott, W. Jin, J. Vuckovi'c, and A.W. Rodriguez, "Inverse design in nanophotonics," Nature Photonics, vol.12, no.11, pp.659–670, Nov. 2018.

[15] J.S. Jensen and O. Sigmund, "Systematic design of photonic crystal structures using topology optimization: Low-loss waveguide bends," Appl. Phys. Lett., vol.84, pp.2022–2024, March 2003.

[16] Y. Tsuji, K. Hirayama, T. Nomura, K. Sato, and S. Nishiwaki, "Design of optical circuit devices based on topology optimization," IEEE Photon. Technol. Lett., vol.18, no.7, pp.850–852, April 2006.

[17] Y. Tsuji and K. Hirayama, "Design of optical circuit devices using topology optimization method with function-expansion-based refractive index distribution," IEEE Photon. Technol. Lett., vol.20, no.12, pp.982–984, June 2008.

[18] N. Uchida, S. Nishiwaki, K. Izui, M. Yoshimura, and T. Nomura, "Topology optimization of electromagnetic waveguides," 8-th World Congress on Structural and Multidisciplinary Optimization, June 2009.

[19] T. Yasui, Y. Tsuji, J. Sugisaka, and K. Hirayama, "Design of three-dimensional optical circuit devices by using topology optimization method with function-expansion-based refractive index distribution," J. Lightw. Techol., vol.31, no.23, pp.3765–3770, Dec. 2013.

[20] Z. Zhang, Y. Tsuji, T. Yasui, and K. Hirayama, "Design of ultra-compact triplexer with function-expansion based topology optimization," Opt. Express, vol.23, no.4, pp.3936–3950, Feb. 2015.

[21] A. Koda, K. Morimoto, and Y. Tsuji, "A study on topology optimization of plasmonic waveguide devices using function expansion method and evolutionary approach," J. Lightw. Technol., vol.37, no.3, pp.981–988, Feb. 2019.

[22] A. Iguchi and Y. Tsuji, "Ultra-small shape-simplified optical diode derived from topology optimal design in plasmonic waveguide," IEICE Electron. Express, vol.16, no.22, 20190598, Nov. 2019.

[23] K. Kudo, K. Morimoto, A. Iguchi, and Y. Tsuji, "A study on optimal design of optical devices utilizing coupled mode theory and machine learning, IEICE Trans. Electron., vol.E103-C, no.11, pp.552–559, Nov. 2020.

[24] M. Tomiyasu, K. Morimoto, A. Iguchi, and Y. Tsuji, "A study on function-expansion-based topology optimization without gray area for optimal design of photonic devices," IEICE Trans. Electron., vol.E103-C, no.11, pp.560–566, Nov. 2020.

[25] T. Bashir, K. Morimoto, A. Iguchi, Y. Tsuji, T. Kashiwa, and S. Nishiwaki, "Optimal design of NRD guide devices using 2D full-vectorial finite element method," IEICE Electron. Express, vol.18, no.15, 20210243, Aug. 2021.

[26] D. Whitley, "A genetic algorithm tutorial," Statist. Comput., vol.4, no.2, pp.65–85, June 1994.

[27] R. Storn and K. Price, "Differential evolution – A simple and efficient heuristic for global optimization over continuous spaces," J. Global Opt., vol.11, no.4, pp.341–359, Dec. 1997.

[28] L. Zhang, L. Liu, X.-S. Yang, and Y. Dai, "A novel hybrid firefly algorithm or global optimization," PLOS One, vol.11, no.9, pp.1–17, Sept. 2016.

[29] Z.W. Geem, "Novel derivative of harmony search algorithm for discrete design variables environmental planning and management program," Appl. Math. Comput., vol.199, no.1, pp.223–230, May 2008.

[30] Y. Tsuji, K. Morimoto, A. Iguchi, T. Kashiwa, and S. Nishiwaki, "Two-dimensional full-vectorial finite element analysis of NRD guide devices," IEEE Micro. Wireless Componen. Lett., vol.31, no.4, pp.345–348, April 2021.

[31] F.L. Texeira and W.C. Chew, "General closed-form PML constitutive tensors to match arbitrary bianisotropic and dispersive linear media," IEEE Microwave Guided Wave Lett., vol.8, pp.223–225, June 1998.

[32] Y. Tsuji and M. Koshiba, "Finite element method using port truncation by perfectly matched layer boundary conditions for optical waveguide discontinuity problems," J. Lightw. Technol., vol.20, no.3, pp.463–468, March 2002.

[33] J.C. Nedelec, "Mixed finite elements in R3," Numer. Math., vol.35, pp.315–341, Sept. 1980.

[34] M. Koshiba and Y. Tsuji, "Curvilinear hybrid edge/nodal elements with triangular shape for guided-wave problems," J. Lightw. Technol., vol.18, no.5, pp.737–743, May 2000.

Yasuhide Tsuji received the B.S., M.S., and Ph.D. degrees in electronic engineering from Hokkaido University, Sapporo, Japan, in 1991, 1993, and 1996, respectively. In 1996, he joined the Department of Applied Electronic Engineering, Hokkaido Institute of Technology, Sapporo, Japan. From 1997 to 2004, he was an Associate Professor of Electronics and Information Engineering at Hokkaido University. From 2004 to 2011, he was an Associate Professor of Electrical and Electronic Engineering at Kitami Institute of Technology, Kitami, Japan. Since 2011, he has been a Professor of Information and Electronic Engineering at Muroran Institute of Technology, Muroran, Japan. He has been interested in wave electronics. Dr. Tsuji is a Senior Member of the Institute of Electronics, Information and Communication Engineers (IEICE), the IEEE, and the Optical Society of America (OSA), and a Member of the Japan Society of Applied Physics. In 2021, He has received the Electronics Society Award form IEICE. In 1997, 1999, and 2019, he was awarded the Best Paper Award from IEICE. In 2000, he has received the Third Millennium Medal from IEEE. In 2019, he has received the IEEE Photonics Technology Letters Outstanding Reviewer Award.

Naoya Hieda received the B.S. degree in department of information and electrical engineering from Muroran Institute of technology, Muroran, Japan, in 2021. He is presently working toward the M.S, degree in Information and Electronic Engineering from Muroran Institute of Technology. Mr. Hieda is a student member of the Institute of Electronics, Information and Communication Engineers (IEICE).

Keita Morimoto received the B.S., M.S., and Ph.D. degrees in information and electronic engineering from the Muroran Institute of Technology, Muroran, Japan, in 2017 and 2019, 2021, respectively, where he is currently a Post-Doctoral Research Fellow of Japan Society for the Promotion of Science (JSPS). Dr. Morimoto is a Member of the Institute of Electronics, Information and Communication Engineers (IEICE) and IEEE.

Akito Iguchi received the B.S., M.S., and Ph.D. degrees in electronic engineering from Muroran Institute of Technology, Muroran, Japan, in 2015, 2017, and 2019. From 2019 to 2020, he was a Post-Doctoral Research Fellow of Japan Society for the Promotion of Science (JSPS). He is currently an Assistant Professor at Muroran Institute of Technology. Dr. Iguchi is a member of the Institute of Electronics, Information and Communication Engineers (IEICE) and IEEE.

Tatsuya Kashiwa was born in Hokkaido, Japan, in 1961. He received the B.S. and M.S. degrees in electrical engineering from Hokkaido University, Sapporo, Japan, in 1984 and 1986, respectively, and the Ph.D. degree. In 1988, he joined the Department of Electrical Engineering as an Assistant Professor. In 1996, he joined the Department of Electrical and Electronic Engineering, Kitami Institute of Technology, as an Associate Professor, where he has been a Professor since 2008. He has co-authored the books Handbook of Microwave Technology (Academic Press), Antennas and Associated Systems for Mobile Satellite Communications (Research Signpost), and Antennas for Small Mobile Terminals (Artech House). His research interests include the analysis of electromagnetic and acoustic fields, electromagnetic compatibility, and optimization problems. He is a member of IEEE and IEEJ. He was a recipient of the IEEE AP-S Tokyo Chapter Young Engineer Award in 1992, IEEJ Technical Development Award in 2019. He was the Chairman of Technical Committee on Electronics Simulation Technology, a member of the Technical Committee on Electromagnetic Theory and Microwaves of IEICE.